ORGANIC CHEMISTRY

FRONTIERS

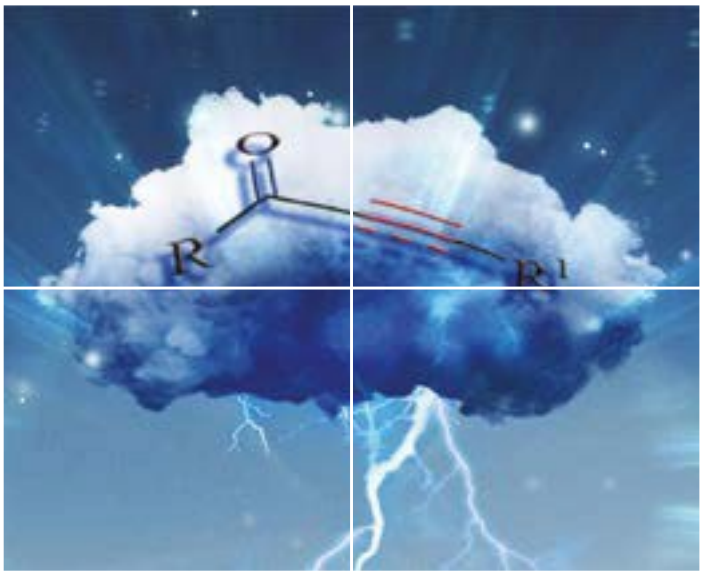

Accepted Manuscript

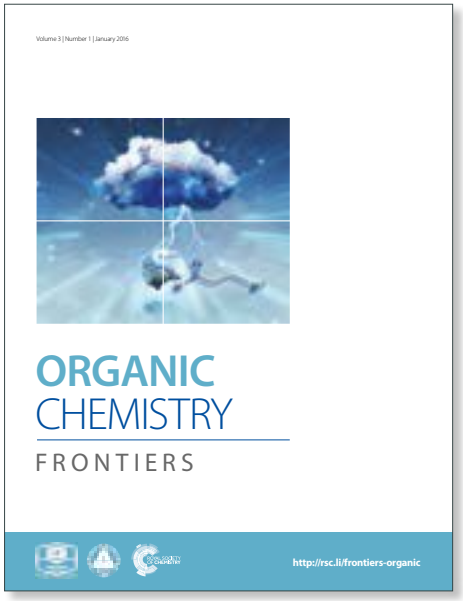

This is an Accepted Manuscript, which has been through the Royal Society of Chemistry peer review process and has been accepted for publication.

Accepted Manuscripts are published online shortly after acceptance, before technical editing, formatting and proof reading. Using this free service, authors can make their results available to the community, in citable form, before we publish the edited article. We will replace this Accepted Manuscript with the edited and formatted Advance Article as soon as it is available.

You can find more information about Accepted Manuscripts in the author guidelines.

Please note that technical editing may introduce minor changes to the text and/or graphics, which may alter content. The journal's standard Terms & Conditions and the ethical guidelines, outlined in our author and reviewer resource centre, still apply. In no event shall the Royal Society of Chemistry be held responsible for any errors or omissions in this Accepted Manuscript or any consequences arising from the use of any information it contains.

Synthesis, Structure, and Property of 5,6,11,12-Tetraarylindeno[1,2-b]fluorenes and Their Applications as Donors for Organic Photovoltaic Devices

Yuan-Chih Lo[a], Hao-Chun Ting[a], Ya-Ze Li[b], Yi-Hua Li[b], Shun-Wei Liu[b,*], Kuo-Wei Huang[c], and Ken-Tsung Wong[a,d*]

[a]Department of Chemistry, National Taiwan University, Taipei 10617, Taiwan.

[b]Department of Electronic Engineering, Ming Chi University of Technology, New Taipei City 24301, Taiwan

[c]KAUST Catalysis Center and Division of Physical Sciences and Engineering, King Abdullah University of Science and Technology, Thuwal 23955-6900, Saudi Arabia

[d] Institute of Atomic and Molecular Science, Academia Sinica, Taipei 10617, Taiwan

Corresponding Author

*(S.-W. Liu) swliu@mail.mcut.edu.tw; (K.-T. Wong) kenwong@ntu.edu.tw

Abstract

The synthesis, structure, and property of three new 5,6,11,12-tetraarylindeno[1,2-*b*]fluorenes are reported. The highly twisted conformations between indeno[1,2-*b*]fluorene core and peripheral aryl substitutions endow these indeno[1,2-*b*]fluorene derivatives good photostability for use as electron donors for vacuum-deposited photovoltaic devices. The optimized device based on **TAInF2** donor blended with C_{70} as electron acceptor produce high open-circuit voltage (> 0.9 V) and a power conversion efficiency of 2.91%. This work demonstrates the first application of indenofluorene derivative as electron donor in organic solar cells.

Organic photovoltaic (OPV) has attracted considerable interests for decades as a promising sustainable approach for transforming sunlight into electrical energy[1–4]. The primary criterion of an organic molecule that can be utilized in OPV is efficient absorption of sun emission. In general, heteroarene-embedded polyaromatic molecules that exhibit strong visible light absorption and promising photostability could be highly potential for OPV application.[5-14] In addition, pure hydrocarbon polyaromatics with extended π-conjugated systems also show good absorption property.[15-21.] However, only limited polycyclic aromatic chromophores with π-conjugated pure hydrocarbon cores have been reported as suitable electronic donors to give good efficiency OPVs[22–26]. Among various pure hydrocarbon polyaromatic structures, indenofluorene (InF)[27,28], a formally anti-aromatic system, exhibits high visible-light absorbance owing to its ground state quinoidal structure[29], could be a good candidate for OPV application. However, some InFs are suspected to form biradical, leading to low stability, which would impede their optoelectronic applications. Recently, independent reports by Haley[30-34] and Yamashita[29], indicated that 6,12-diarylindeno[1,2-*b*]fluorenes are stable. Particularly, indeno[1,2-*b*]fluorene derivatives with highly twisted aryl substitutions at C6 and C12 positions showed remarkable photostability, which is crucial for further application. In addition, the carrier transport characters of indeno[1,2-*b*]fluorene derivatives also suggest high potential for optoelectronic application[29,30]. As reported, the introduced aryl substitutions can effectively govern structural stability and modulate the physical properties of indeno[1,2-*b*]fluorene derivatives[29-32]. A key factor for the structural stability is the dihedral angle between the peripheral aryl group and coplanar indeno[1,2-*b*]fluorene core. We envisioned additional aryl substitutions introduced at C5 and C11 of the indeno[1,2-*b*]fluorene core should significantly twist C6 and C12 aryl substituents, leading to more photostable indeno[1,2-*b*]fluorene derivatives. To the best of our knowledge, the synthesis and property of 5,6,11,12-tetraaryl-substituted indeno[1,2-*b*]fluorenes have not been reported. In this work, we report the synthesis, X-ray structure, and properties of three new 5,6,11,12-tetraarylindeno[1,2-*b*]fluorenes (**TAInF1–3**, Scheme 1), and compare them to those of 6,12-diphenylindeno[1,2-*b*]fluorene to demonstrate the effects of C5 and C11 aryl substituents on structural features and physical characteristics. These new tetraaryl InF derivatives were further utilized as electron donors blended with C_{70} as active layer in vacuum-

processed bulk heterojunction (BHJ) organic solar cells (OSCs). The device employing **TAInF2** as electron donor exhibited the best performance with power conversion efficiency (PCE) of up to 2.91%. Our results manifested the first example and potential of using indenofluorene as electron donor in OPV applications.

Scheme 1. Synthesis of TAInF1–3.

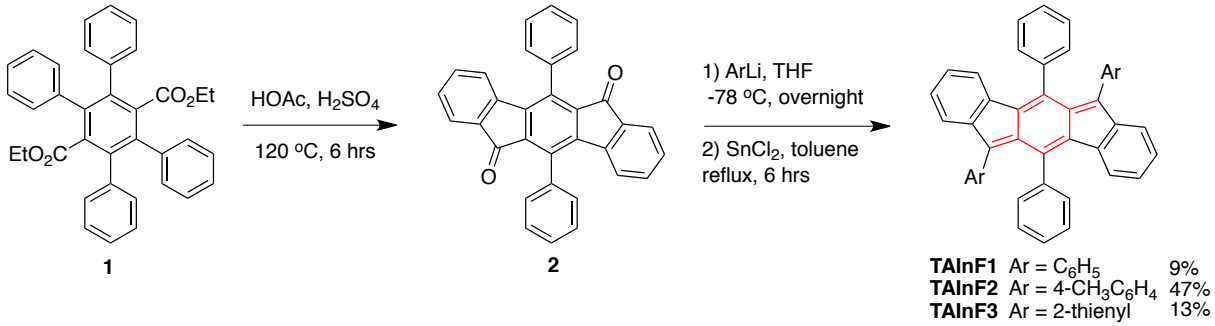

Scheme 1 depicts the synthesis of 5,6,11,12-tetraarylindeno[1,2-*b*]fluorenes (**TAInF**). Following the protocols established by Haley and Yamashita[29,30], the nucleophilic addition of appropriate aryl lithium to an indenofluorenone (**2**), which was prepared according to the reported literature from the diester (**1**)[35], produced corresponding diol intermediates. The crude diols were reduced with $SnCl_2$ in refluxing toluene to furnish the target molecules with low isolated yields because of the low solubility in organic solvents.

Single crystals of **TAInF1**–**3**, suitable for X-ray analysis, were obtained from a bilayer ($CHCl_3$/MeOH) diffusion method. The crystal structures are shown in Figure 1 and crystal data are summarized in Table S1 (Electronic Supplementary Information, ESI). The selected bond lengths of InF cores are listed in Figure 1 (also Table S1 in ESI). The bond length alternations (BLA) are observed in all cases, indicating a quinoidal core structure in the ground state. Interestingly, the external C_1=C_2 bonds are slightly longer than internal C_9=C_{10} bonds in 6,12-diphenyl and -ditolyl substituted InFs, **TAInF1** and **TAInF2**, respectively, which are similar to reported cases of 6,12-diarylindeno[1,2-*b*]fluorenes. Whereas, the external and internal C=C bonds of quinoidal core are same length in thiophene-substituted InF (**TAInF3**). The dihedral angle between C5, C11-substituted phenyl rings and the central phenylene ring of InFs were calculated to be 73.2°–79.5° (Figure 1).

Apparently, the steric congestion from C5- and C11-substituted phenyl rings forces the C6 and C12 aryl substitutions to adopt highly twisted conformation with large dihedral angles of 63.8° to 66.8°, which are larger than the case of 6,12-diphenylindeno[1,2-*b*]fluorene (43.4°) and close to those of analogous 6,12-diarylindeno[1,2-*b*]fluorenes (56.6–76.5°)[5] showing higher photostability. This implies that the introduction of phenyl substitutions onto the central phenylene ring of InF imparts the ability to twist C6- and C12-substituted aryl groups, which is the crucial factor governing molecular stability.

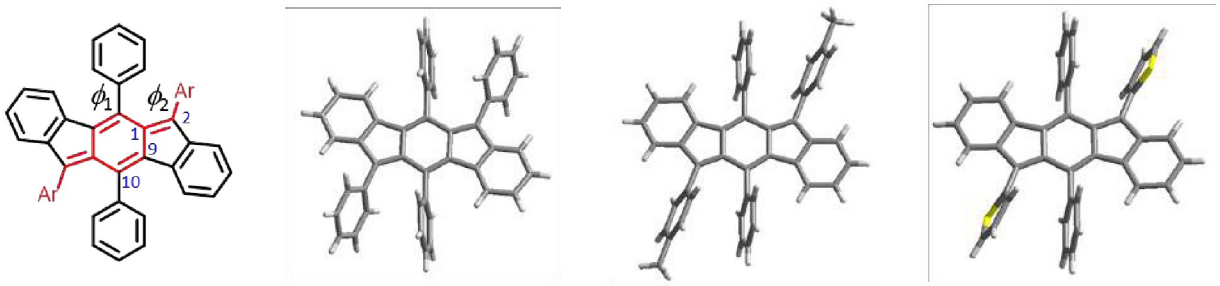

	TAInF1	TAInF2	TAInF3
Ar =	phenyl	p-tolyl	2-thienyl
ϕ_1	79.51(5)°	74.51(8)°	73.22(10)°
ϕ_2	64.82(6)°	66.80(8)°	63.76(10)°
C_1=C_2 (Å)	1.389(2)	1.390(3)	1.384(4)
C_9=C_{10} (Å)	1.365(2)	1.363(3)	1.377(4)

Figure 1. X-ray structures of **TAInF1–3** and relevant dihedral angles of peripheral aryl substituents relative to the InF core and selected bond lengths.

It is generally accepted that molecular ordering has a pronounced effect on charge carrier transport behavior. The crystals of **TAInF1** and **TAInF3** adopted a brick wall-like packing motif mediated through evident π-π stacking interactions (Figure 2). In contrast, a herringbone-type packing was observed in **TAInF2** crystals. Clearly, the extra space demand of the methyl terminus in **TAInF2** led to less-ordered packing in crystals. Thermogravimetric analysis (TGA) indicated these new tetraarylindeno[1,2-*b*]fluorenes exhibited relatively high thermal stability, with decomposition temperature (T_d) (corresponding to 5% weight loss) higher than 318 °C (Table 1), producing sufficient stability for thermal deposition under a high vacuum.

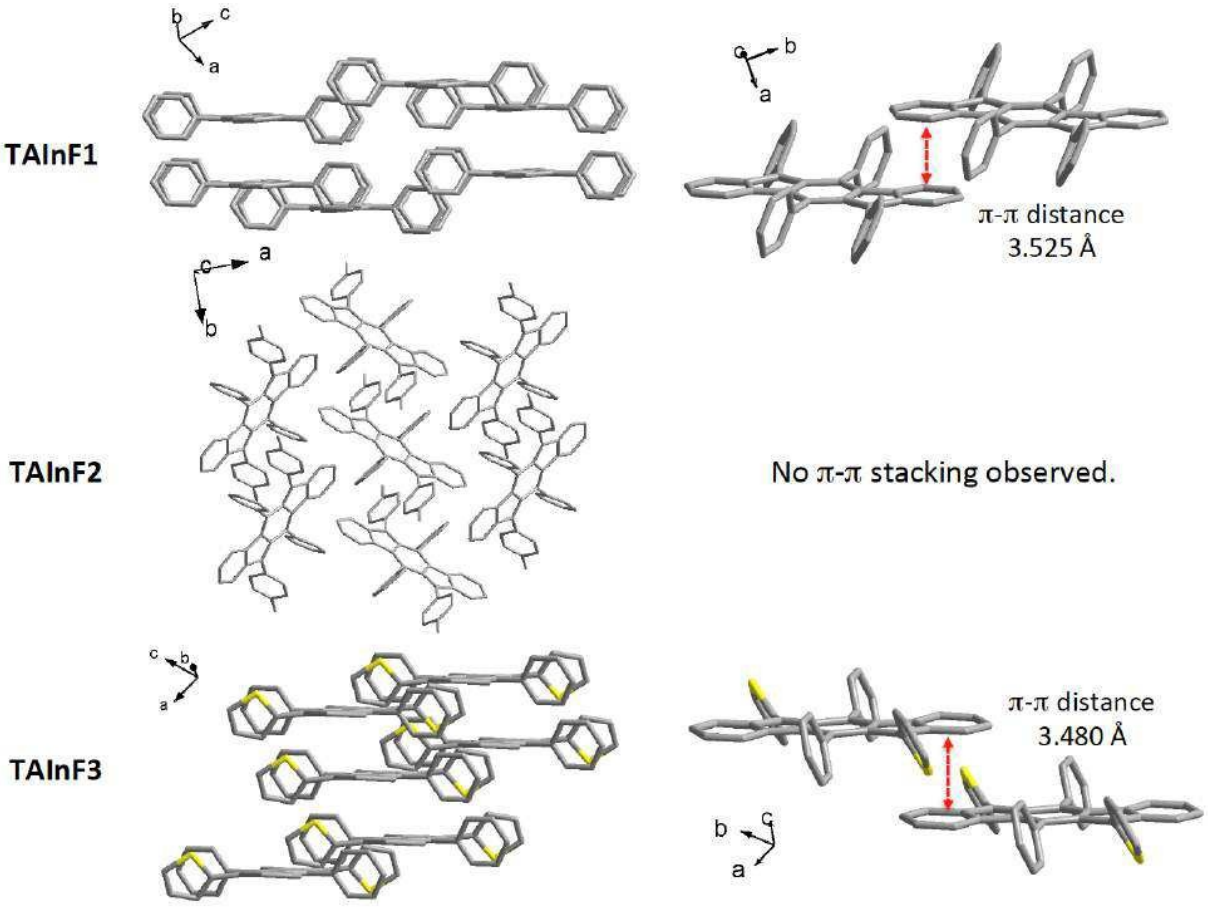

Figure 2 Crystal packing of **TAInF1–3** and π−π interactions of **TAInF1** and **TAInF3.**

The electronic absorption spectra of **TAInF1–3** in dichloromethane are shown in Figure 3 and the data are summarized in Table 1. These compounds exhibited a broad absorption band with vibronic features and notably high extinction coefficient (3.5–4.2 × 10^4 $M^{-1}cm^{-1}$) in the visible wavelength region (450–600 nm). The λ_{max} of thiophene-substituted **TAInF3** was slightly red-shifted (~40 nm) as compared to those of **TAInF1** and **TAInF2**. Interestingly, the λ_{max} of 5,6,11,12-tetraphenylindeno[1,2-*b*]fluorene (**TAInF1**) was blue-shifted (~20 nm) as compared to that of 6,12-diphenylindeno[1,2-*b*]fluorene. DFT calculations were able to reproduce the molecular structures (Figure 4), and orbital analysis indicated that HOMO and LUMO were localized on the InF core with limited contribution from C6 and C12 aryl substitutions and neglected contribution from C5 and C11 phenyl group. Hence, the highly twisted conformations decoupling the π-conjugations between InF core and peripheral aryl substitutions account for larger optical energy gaps of tetraaryl-substituted InFs.

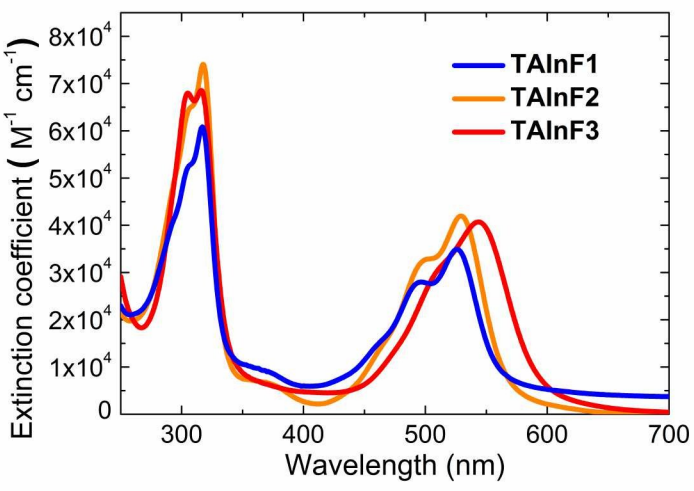

Figure 3. UV-Vis absorption spectra of **TAInF1–3** measured in CH_2Cl_2.

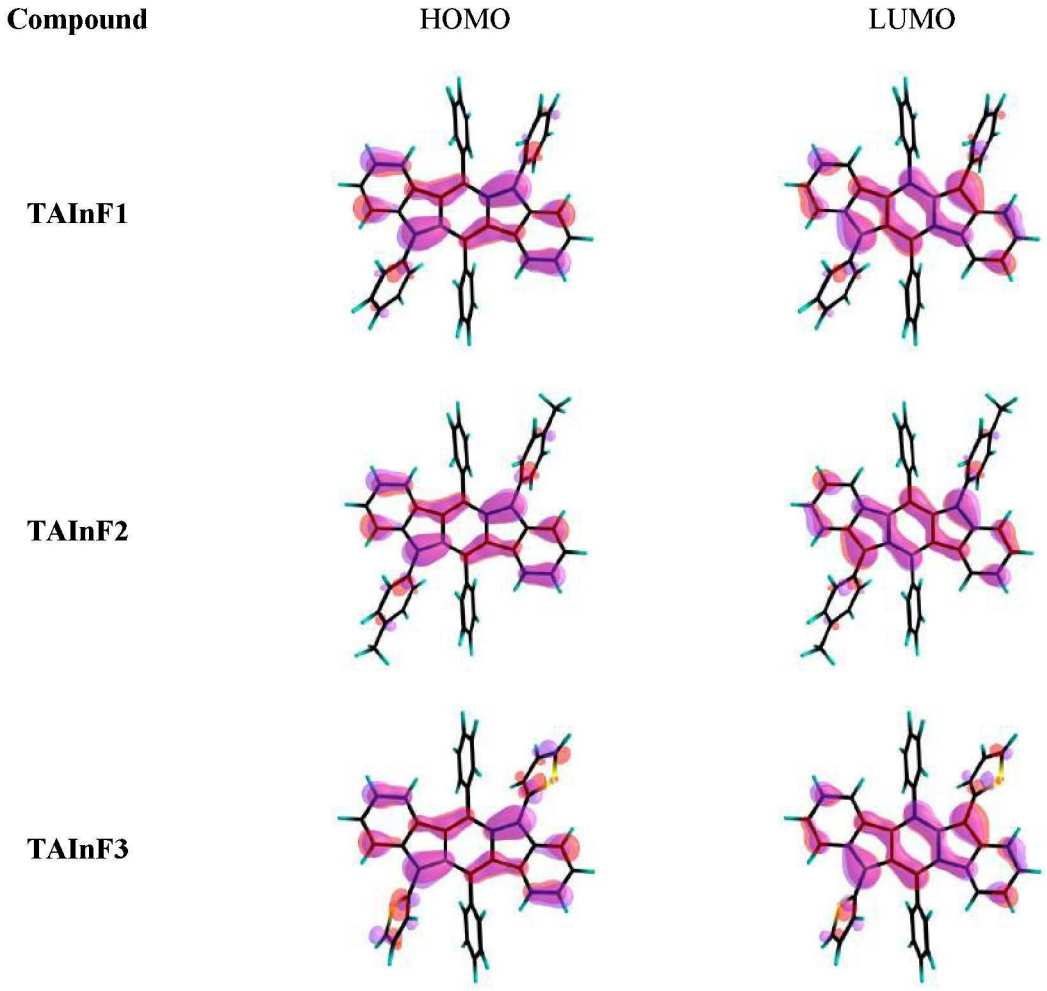

Figure 4 Calculated HOMO and LUMO of **TAInF1–3**

Table 1. Physical Properties of New 5,6,11,12-tetraarylindeno[1,2-*b*]fluorenes (**TAInF1–3**).

Compound	λ_{abs} sol. (nm)[a] (ε, $M^{-1}cm^{-1}$)	λ_{abs} film[b] (nm)	ΔE^{opt} (sol.)[a] (eV)	ΔE^{opt} (film)[b] (eV)	$E_{1/2}^{ox}$ (V)	$E_{1/2}^{red}$ (V)	ΔE^{CV} (eV)	HOMO/LUMO (eV)[c]	Td (°C)[d]
TAInF1	557 (34900)	530	2.23	2.05	0.574	-1.54	2.11	−5.37/−3.26	335
TAInF2	571 (42000)	544	2.18	2.03	0.479	-1.61	2.09	−5.28/−3.19	325
TAInF3	598 (40700)	590	2.08	1.81	0.452	-1.44	1.89	−5.25/−3.36	318

[a]Measured in CH_2Cl_2 solution (10^{-5} M) and the value was estimated from the onset. [b]Thin film on quartz substrate. [c]Estimated from the HOMO (−4.8 eV) of ferrocene using Fc^+/Fc redox couple as reference. [d]Temperature corresponding to 5% weight loss obtained from TGA analysis.

The electrochemical property of **TAInF1–3** was probed with cyclic voltammetry (CV). The CV curves (Figure 5) clearly reveal the reversibility of oxidation (in CH_2Cl_2) and reduction (in THF) scans, indicating electrochemical stability of the corresponding ionic radicals. The oxidation potentials (~0.9 V vs. Ag/AgCl) of these 5,6,10,11-tetraarylindeno[1,2-*b*]fluorenes were independent of the structural features of aryl substitutions, whereas the reduction potential of **TAInF3** was surprisingly lower than those of diphenyl- and ditolyl-substituted counterparts (**TAInF1** and **TAInF2**). Theoretical analysis showed **TAInF3** was also found to be 3–4 kcal/mol more favorable for reduction than **TAInF1** or **TAInF2**, consistent with experimental observations. Evaluation of the singly occupied orbitals of three anion radicals (all similar with the electron density shared by the thiophene and phenyl groups in **TAInF1–3**, Figure S1 in ESI) suggested the difference may be due to the tendency of thiophene and phenylene rings to be reduced. In all cases, no singlet biradical character was identified computationally or experimentally, suggesting they all have closed-shell ground state structures. The HOMO and LUMO energy levels of **TAInF1–3** were estimated from the HOMO (−4.8 eV) of ferrocene (Fc) as Fc^+/Fc redox couple served as reference (Table 1). Clearly, the red-shifted λ_{max} of **TAInF3** was attributable to a lower LUMO than those of diphenyl- and ditolyl-substituted counterparts.

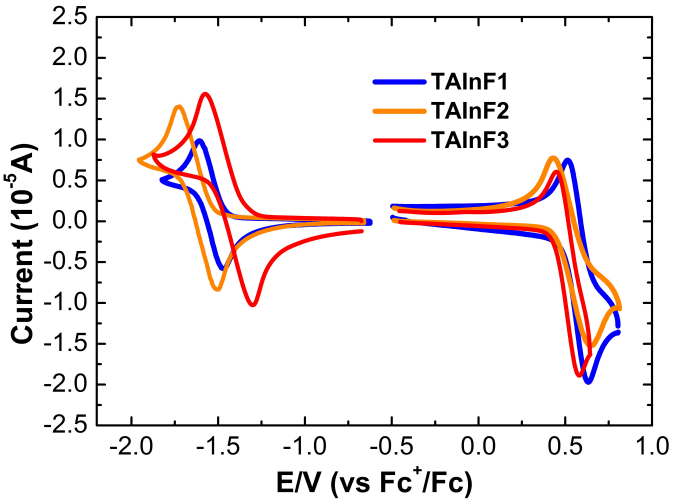

Figure 5. Cyclic voltammogram of **TAInF1**–**3**.

The thin films of **TAInF1**–**3** exhibited red-shifted λ_{max} and wide visible-light absorption covering from 400 to 700 nm (Figure S2 in ESI), which can facilitate efficient sunlight harvesting. The ionization potential (IP) of **TAInF1**–**3** thin film was determined by AC-2 (Figure S3 in ESI). The low-lying IPs ~5.6 eV, together with broad absorption, implies these new tetraarylindeno[1,2-*b*]fluorenes have potential applications as small molecule electron donors for vacuum-deposited OPVs.

Owing to the high crystalline feature, these new tetraarylindeno[1,2-*b*]fluorenes were first employed as donor materials in vacuum-processed bilayer-type OPVs configured as ITO/ MoO_3 (15 nm)/ **TAInF1–3** (12 nm)/ C_{60} (50 nm)/ BCP (8 nm)/ Ag (120 nm), where bathocuproine (BCP) was introduced as an electron-transporting and hole-blocking layer. Device performances are summarized in Figure S4 and Table S2. The PCE of these bilayer-type OPVs was only 0.31, 0.47, and 0.41% for **TAInF1**, **TAInF2**, and **TAInF3**-based devices, respectively. The low PCEs were attributed to limited donor/acceptor interfaces, where the relatively thick C_{60} layer was mainly responsible for absorbing visible light and generating the exciton. The obtained open-circuit voltage (Voc) value, **TAInF1** (0.54 V), **TAInF2** (0.63 V), and **TAInF3** (0.62 V), were nonetheless significantly lower than the energy level differences between the IPs (**TAInF1**: 5.70 eV, **TAInF2**: 5.65 eV, and **TAInF3**: 5.60 eV) and the LUMO level of C_{60} (4.4 eV)[26]. Our previous work demonstrated the Voc strongly depends on the electron donor's morphology and intermolecular interaction[36], implying the structural features of

tetraarylindeno[1,2-*b*]fluorenes, in addition to different intermolecular interactions, may dramatically affect Voc. The pure **TAInF1–3** films were then probed with an atomic force microscope (AFM) to explore the effects of molecular packing on surface morphology. Figure 6 shows the surface roughness of herringbone-packing **TAInF2** film was relatively smooth (rms = 0.525 nm). In contrast, **TAInF3** (rms = 3.562 nm) and **TAInF1** (rms = 15.12 nm), which adopted brick wall-like packing motif in crystals, exhibited rough surface morphology. The rough surface morphology of **TAInF1** film resulted in lowest Voc among donors, because of strong intermolecular interactions or aggregations. This implies that suppressing the propensity of intermolecular interactions or aggregations of crystalline tetraarylindeno[1,2-*b*]fluorenes is crucial for improving OPV device characteristics. Thus, vacuum-deposited bulk heterojunction (BHJ) OPVs with active layers of **TAInF1–3**:C_{70} blended films were fabricated with the device configured as ITO/ MoO_3 (15 nm)/active layer (1:1 by volume, 45 nm)/ BCP (8 nm)/Ag (120 nm). Figure 7 shows the JV characteristics of BHJ OPV devices. Device performance data are summarized in Table S3. However, in spite of superior exciton dissociation in BHJ devices with InF/C_{70} (1:1) blended active layer, the obtained Jsc and PCE were only slightly improved over those of bilayer-type devices (Table S2 in ESI). Nevertheless, the Voc of **TAInF1**:C_{70} (1:1) BHJ OPV (0.90 V) was much higher than that of **TAInF1-**based bilayer-type OPV (0.54 V). AFM analysis indicated smooth surface roughness of **TAInF1–3**:C_{70} thin films (Figure S5 in ESI), implying the intermolecular interactions or aggregations of crystalline tetraarylindeno[1,2-*b*]fluorenes were suppressed as they mixed with C_{70}, thereby reducing the reverse saturation current of the device, resulting in high Voc. The low device efficiency was possibly because, even with 1:1 mixing ratio, the active layer could not provide greater charge balance/collection efficiency or sufficient absorption (Figure S4 in ESI). Tang reported that bulk OPV active layer with a low donor concentration can achieve high PCE owing to high absorption and charge collection capability of the C_{70} acceptor[37]. Accordingly, BHJ OPV devices with a low tetraarylindeno[1,2-*b*]fluorene ratio were examined. The device based on **TAInF2**:C_{70} (1:10) as active layer achieved a superior PCE of 2.91% with Voc of 0.94 V, Jsc of 8.62 mA/cm^2, and FF of 35.9%, under standard AM 1.5 irradiation, whereas **TAInF1-** and **TAInF3**-based devices achieved 1.7% PCE (Figure S6 and Table S3 in ESI). The improved performance was ascribed to the

formation of well-separated donor/acceptor phases in the low-donor-concentration **TAInF2**:C_{70} active layer.

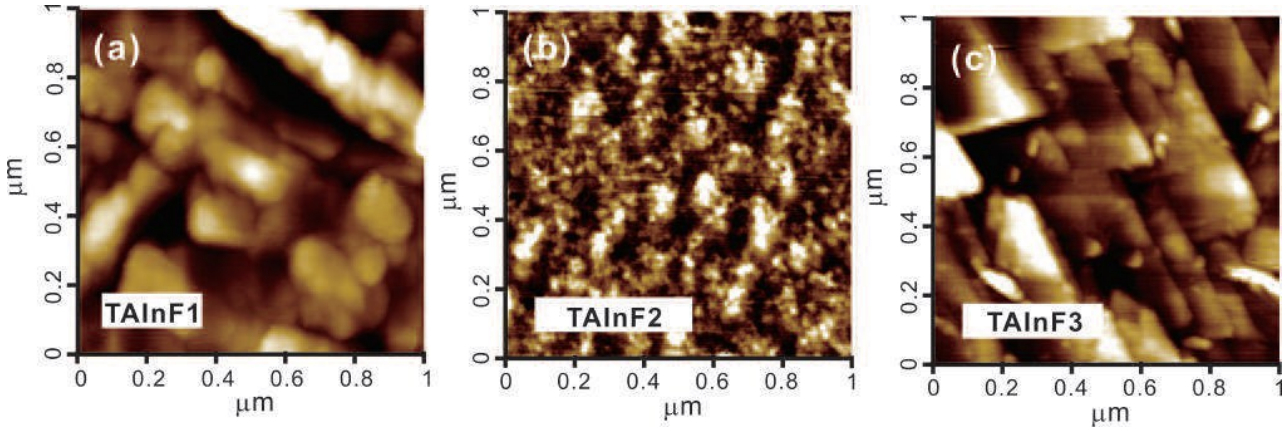

Figure 6. AFM images of 30 nm (a) **TAInF1**, (b) **TAInF2**, and (c) **TAInF3** thin films on Si wafers. The root mean square (rms) roughness was obtained from an area of 1 μm × 1 μm.

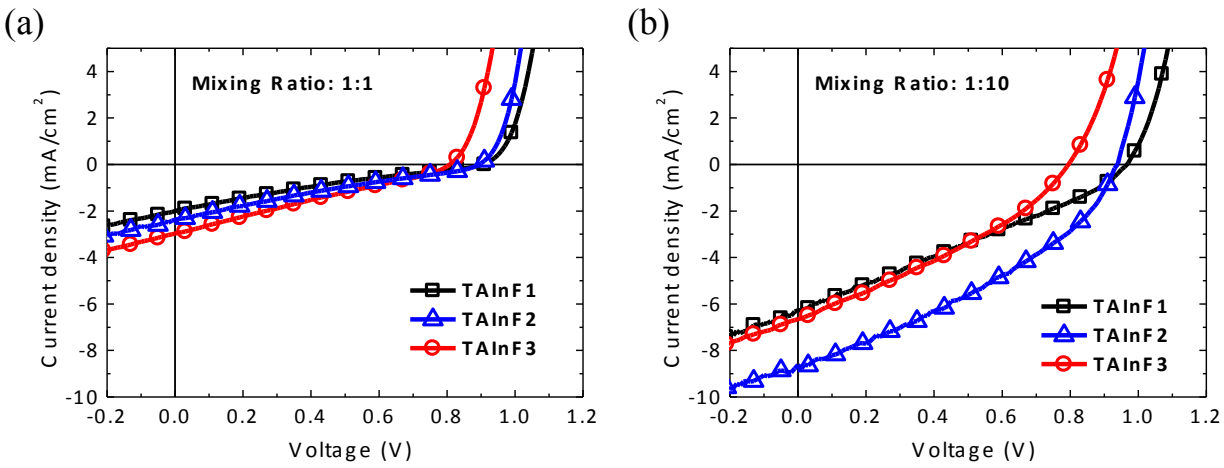

Figure 7. Electrical characteristics of **TAInF1**:C_{70} (square), **TAInF2**:C_{70} (triangle), and **TAInF3**:C_{70} (circle) bulk heterojunction OPVs with active layer of (a) 1:1 and (b) 1:10 mixing ratio.

In summary, three new 5,6,11,12-tetraarylindeno[1,2-*b*]fluorenes were synthesized and characterized. X-ray structural analyses indicated the additional aryl substitutions introduced at C5 and C11 of InF core significantly twisted C6 and C12 phenyl substituents, which is the crucial factor for molecular stability. The highly twisted conformations decoupled the π-conjugations between the InF core and peripheral aryl substitutions led to blue-shifted absorption, compared to that of 6,12-diphenylindeno[1,2-*b*]fluorene. Theoretical analyses also confirmed that both HOMO/LUMO

orbitals were mainly localized on the InF core with limited contribution from C6 and C12 aryl substitutions, neglecting contribution from C5 and C11 aryl groups. In all cases, no singlet biradical character was identified computationally or experimentally, suggesting they all have closed-shell ground state structures. The low-lying IPs ~5.6 eV, together with broad absorption, made these new tetraarylindeno[1,2-*b*]fluorenes suitable electron donors for vacuum-deposited OPVs. The superlative device adopted **TAInF2** blended with C_{70} as donor and acceptor, respectively, in the active layer, achieving power conversion efficiency (PCE) of up to 2.91%. Our results manifest the effects of C5- and C11-aryl substitutions on structural features and physical characteristics of InF derivatives and pioneer the use of indenofluorene as electron donor in OPV applications.

Electronic Supplementary Information

Detailed experimental procedures for synthesis and characterization of new compounds, device fabrication and measurement of OPV devices, crystal data and packing, theoretical calculations, film absorption spectra, photoelectron spectroscopy, OPVs device characteristics and AFM images of **TAInF1–3:**C_{70} films as a PDF file. The Electronic Supplementary Information is available free of charge on the RSC Publications website.

Acknowledgment

The authors acknowledge financial support from the Ministry of Science and Technology Taiwan (Grant Nos. 104-2113-M-002-006-MY3 and 104-2119-M-131-001).

References

(1) H. Zhou, L. Yang and W. You, *Macromolecules* 2012, **45**, 607.

(2) Y. Lin, Y. Li and X. Zhan, *Chem. Soc. Rev.* 2012, **41**, 4245.

(3) X. Zhan, A. Facchetti, S. Barlow, T. J. Marks, M. A. Ratner, M. R. Wasielewski and S. R. Marder, *Adv. Mater.* 2011, **23**, 268.

(4) A. Mishra and P. Bauerle, *Angew. Chem. Int. Ed.* 2012, **51**, 2020.

(5) Ye, Q.; Chang, J.; Shi, X.; Dai, G.; Zhang, W.; Huang, K. W.; Chi, C. *Org. Lett.* 2014, **16**, 3966.

(6) Yue, W.; Suraru, S. L.; Bialas, D.; Muller, M.; Wurthner, F. *Angew. Chem. Int. Ed.* 2014, **53**, 6159.

(7) Marek Grzybowski, E. G.-M., Tomasz Stoklosa, Daniel T. Gryko *Org. Lett.* 2012, **14**, 2670.

(8) Bunz, U. H. *Acc. Chem. Res.* 2015, **48**, 1676.

(9) Liang Z., Tang Q., Xu J., Miao Q. *Adv. Mater.* 2011, **23**, 1535.

(10) Hahn, S.; Geyer, F. L.; Koser, S.; Tverskoy, O.; Rominger, F.; Bunz, U. H. *J. Org. Chem.* 2016, **81**, 8485.

(11) Matsuo, K.; Saito, S.; Yamaguchi, S. *J. Am. Chem. Soc.* 2014, **136**, 12580.

(12) Miao, Q. *Adv. Mater.* 2014, **26**, 5541.

(13) Saito, S.; Matsuo, K.; Yamaguchi, S. *J. Am. Chem. Soc.* 2012, **134,** 9130.

(14) Zeng, Z.; Ishida, M.; Zafra, J. L.; Zhu, X.; Sung, Y. M.; Bao, N.; Webster, R. D.; Lee, B. S.; Li, R. W.; Zeng, W.; Li, Y.; Chi, C.; Lopez Navarrete, J. T.; Ding, J.; Casado, J.; Kim, D.; Wu, J. *J. Am. Chem. Soc.* 2013, **135**, 6363.

(15) Konishi, A.; Hirao, Y.; Matsumoto, K.; Kurata, H.; Kubo, T. *Chem. Lett.* 2013, **42**, 592.

(16) Gu, X.; Xu, X.; Li, H.; Liu, Z.; Miao, Q. *J. Am. Chem. Soc.* 2015, **137**, 16203.

(17) Li Z., Du J., Tang Q., Wang F., Xu J., Yu J. C., Miao Q. *Adv. Mater.*, 2010, **22**, 3242–3246.

(18) Hsieh, Y. C.; Wu, T. C.; Li, J. Y.; Chen, Y. T.; Kuo, M. Y.; Chou, P. T.; Wu, Y. T. *Org. Lett.* 2016, **18**, 1868.

(19) Hu, P.; Lee, S.; Park, K. H.; Das, S.; Herng, T. S.; Goncalves, T. P.; Huang, K. W.; Ding, J.; Kim, D.; Wu, J. *J. Org. Chem.* 2016, **81**, 2911.

(20) Rudiger, E. C.; Rominger, F.; Steuer, L.; Bunz, U. H. *J. Org. Chem.* 2016, **81**, 193.

(21) Yang, X.; Liu, D.; Miao, Q. *Angew. Chem. Int. Ed.* 2014, **53**, 6786.

(22) L. Zhang, Y. Cao, N. S. Colella, Y. Liang, J. L. Bredas, K. N. Houk and A. L. Briseno, *Acc. Chem. Res.* 2015, **48**, 500.

(23) S. Yoo, B. Domercq and B. Kippelen, *Appl. Phys. Lett.* 2004, **85**, 5427.

(24) C.-W. Chu, Y. Shao, V. Shrotriya and Y. Yang, *Appl. Phys. Lett.* 2005, **86**, 243506.

(25) O. L.; Griffith and S. R. Forrest, *Nano letters* 2014, **14**, 2353.

(26) L. Zhang, B. Walker, F. Liu, N. S. Colella, S. C. B. Mannsfeld, J. J. Watkins, T.-Q. Nguyen and A. L. Briseno, *J. Mater. Chem.* 2012, **22**, 4266.

(27) Shimizu, A.; Kishi, R.; Nakano, M.; Shiomi, D.; Sato, K.; Takui, T.; Hisaki, I.; Miyata, M.; Tobe, Y. *Angew. Chem. Int. Ed.* 2013, **52**, 6076.

(28) Shimizu, A.; Tobe, Y. *Angew. Chem. Int. Ed.* 2011, **50**, 6906.

(29) J. Nishida, S.; Tsukaguchi and Y. Yamashita, *Chem. Eur. J.* 2012, **18**, 8964.

(30) D. T. Chase, A. G. Fix, S. J. Kang, B. D. Rose, C. D. Weber, Y. Zhong, L. N. Zakharov, M. C. Lonergan, C. Nuckolls and M. M. Haley, *J. Am. Chem. Soc.* 2012, **134**, 10349.

(31) D. T. Chase, A. G. Fix, B. D. Rose, C. D. Weber, S. Nobusue, C. E. Stockwell, L. N. Zakharov, M. C. Lonergan and M. M. Haley, *Angew. Chem. Int. Ed.* 2011, **50**, 11103.

(32) D. T. Chase, B. D. Rose, S. P. McClintock, L. N. Zakharov and M. M. Haley, *Angew. Chem. Int. Ed.* 2011, **50**, 1127.

(33) B. D. Rose, N. J. Sumner, A. S. Filatov, S. J. Peters, L. N. Zakharov, M. A. Petrukhina and M. M. Haley, *J. Am. Chem. Soc.* 2014, **136**, 9181.

(34) G. E. Rudebusch, A. G. Fix, H. A. Henthorn, C. L. Vonnegut, L. N. Zakharov and M. M. Haley, *Chem. Sci.* 2014, **5**, 3627.

(35) M. Samuel, B. Maria and Z. Y. Wang, *Org. Lett.,* 2002, **4**, 2157.

(36) S.-W. Liu, W.-C. Su, C.-C. Lee, C.-F. Lin, C.-W. Cheng, C.-C. Chou, J.-H. Lee and C.-T. Chen, *Sol. Energy Mater. Sol. Cells* 2013, **109**, 280.

(37) M. Zhang, H. Wang, H. Tian, Y. Geng and C. W. Tang, *Adv. Mater.* 2011, **23**, 4960.